Pergamon

Int. J. Heat Mass Transfer. Vol. 40, No. 8, pp. 1951–1961, 1997

0017–9310/97 $17.00+0.00

PII: S0017–9310(96)00236–0

Homogeneous turbulence evolution in stably stratified flow—I. Internal gravity waves at low inverse Froude numbers

V. A. BABENKO

The Luikov Heat and Mass Transfer Institute of the Academy of Science, Minsk, Belarus

(*Received* 23 *February* 1995)

Abstract—The evolution of homogeneous grid-generated turbulence in stratified fluid is investigated analytically. A small parameter decomposition on inverse Froude number is applied to the theory of nearly homogeneous turbulence developed earlier in refs. [1] and [2]. Applying the multiple scale method we calculate the frequency and amplitude of internal gravity waves and formulate differential system describing the wave-averaged behaviour of turbulence characteristics. The comparison with the numerical results published in [2] and with known experimental data shows a very good agreement as to internal waves as to small scale turbulence in collapsed state. The long-term turbulence evolution in weakly stratified media can be regarded as a singular perturbation problem permitting us to gain an insight into the interaction between gravity waves and active turbulence.

1. INTRODUCTION

Turbulence in stably stratified fluid has been a subject of intensive investigation over the last two decades. The interest in the problem was stimulated by the practical importance of mixing processes in the ocean and the atmosphere. This problem has been investigated experimentally in laboratory conditions (in salt water tanks and wind tunnels) and in natural observations. Numerical modelling has been made on the basis of Navier–Stokes equations (direct numerical simulation) or on the basis of second order models.

Turbulence evolution in a stratified flow differs essentially from one in a non-stratified fluid, due to the presence of additional buoyancy mechanism of transfer, production and dissipation of turbulence kinetic energy (TKE). In a stably stratified fluid small scale turbulence can fully or partially turn into internal gravity waves. The separation of the active turbulence and the wave motion in oceanic flows is of importance for the interpretation of oceanographic experiments and the determination of such practical matters as vertical flux of mass and mixing efficiency.

The main effect of gravity on stratified flow is in shrinking the turbulent wake vertically; in view of this, viscous forces suppress the turbulent motion more rapidly. As a consequence, turbulence goes into a so called 'collapsed state' [3] in which TKE is converted into the potential energy of density fluctuations, $P = \frac{1}{2}\rho^2/N^2g^2/\rho$, where $N = (g/\bar{\rho}\,\mathrm{d}\bar{\rho}/\mathrm{d}x_2)^{1/2}$ is the Brunt–Väisälä frequency, that is the frequency of internal waves in a stable atmosphere. The onset of fossilization is detected in experiments as a sharp decrease of the rate of TKE decay and a stop in the growth rate of mixing layer thickness [4, 5]. A review of a considerable number of papers dealing with the collapsed state was contributed by Hopfinger [6]. Criteria of the collapse onset was also considered in detail in refs. [4, 7] and in works of the Van Atta group [5, 8, 9].

Collapsed state has been intensively studied in shear free and shear flows. The mean shear was not found to be of essential importance provided that the global Richardson number is less than 0.1,

$$Ri_g = g\frac{\Delta\rho}{\bar{\rho}}\frac{\delta}{(\Delta U)^2}$$

where $\Delta\rho$ and ΔU are density and velocity differences across the layer, δ the layer thickness, $\bar{\rho}$ the mean density. In oceanic observations the shear is usually small, so the results of laboratory experiments and of direct numerical simulation (DNS) appear to have a strong relationship to the situation which really exists in the atmosphere and in the ocean [6].

The turbulence structure in the collapsed state (two-dimensional turbulence, internal waves or both) has also been investigated by many authors. While the mean effect of buoyancy was found to suppress the vertical velocity fluctuations and in some earlier papers collapse was treated as a full abrupt stop of vertical fluctuations, later in numerical studies [10–14] and in laboratory experiments [8, 9] it was detected that the transition to 2-D turbulence has an oscillatory character. It was pointed out that only a small fraction of TKE can be converted into the potential energy of density fluctuations irreversibly [6]. Such a situation appears to take place in the ocean where the efficiency of vertical mixing even at very long evolution time is essentially higher than that due to the molecular

NOMENCLATURE

$E = \overline{u_i^2}/U^2$ dimensionless kinetic energy
$F = NM/U$ inverse Froude number
M cell size of a grid
$N = (g\,\mathrm{d}\bar{\rho}/\rho\,\mathrm{d}x_2)^{1/2}$ Brunt–Väisälä number
$Q = (-\overline{u_2\rho}/(UM^{\mathrm{d}\bar{\rho}}/\mathrm{d}x_2)$ dimensionless turbulent transverse mass flux
$R_{22} = \overline{u_2^2}/U^2$ vertical component of velocity pulsation tensor
$R_\lambda = (5ET_uRe)^{1/2}$ turbulent Reynolds number
$Re = UM/\nu$ Reynolds number
$T_\rho = (\overline{\rho^2}U)/(\varepsilon_\rho M)$ time scale of density field
$T_u = (\overline{u_i^2}U)/(\varepsilon_u M)$ time scale of velocity field
U flow velocity
$\overline{u_i^2}$ doubled turbulence kinetic energy.

Greek symbols
$\varepsilon = F^2$ small parameter
ε_ρ dissipation rate of density fluctuations
ε_u dissipation rate of velocity fluctuations
σ molecular Prandtl number
$\tau = \tau^* U/M$ dimensionless time
$\hat{\tau} = \sqrt{\varepsilon}\tau = N\tau^*$, $t = \varepsilon T_\rho$ fast and slow time variables
τ^* dimensionless time
$\Theta = \overline{\rho^2}/(M^{\mathrm{d}\bar{\rho}}/\mathrm{d}x_2)^2$ squared density fluctuation.

diffusion. Stratification primarily influences disturbances with large scales, while small-scale fluctuations and turbulent mixing at small scales are still possible at any evolution time.

Riley [11] supposed that 2-D waves and quasi 2-D turbulent motion coexist at different scales. Lilly [12] developed this idea in more detail with the assumption that spatial scales in stratified flow are approximately isotropic, but velocity scales essentially differ. This led him to introduce two different time scales: one for internal waves, N^{-1}, and another for turbulent motion, L/u', where L is integral length scale and u' is r.m.s. velocity. As a results two various sets of equations were obtained. The idea of a two-scale character of stratified flow was firmly confirmed by experimental investigation, see ref. [9]. Numerical calculations in ref. [14] for conditions of experiments in ref. [9] also showed the presence of oscillations in kinetic and potential energies and also in various length scales.

In the cited works the frequency of internal waves was found to be approximately two-fold greater than the Brunt–Väisälä number N. The time scale N^{-1} represents the upper limit for the period of internal waves generated in a stratified fluid by buoyancy effects. It lets us generalize many of the buoyancy driven features of the flow. For instance, the time of the collapse onset in the most of laboratory experiments and DNS runs was within an interval $N\tau^* = 1.5$–2.5, the period of oscillations was in interval $N\tau^* = 3$–4. However, it was not possible to say anything about distribution of energy between internal waves and active small-scale turbulence [6].

Another time scale in the given problem, is determined by the ratio L/U, where L is some internal length scale in the flow (grid size M in experiments with grid-generated turbulence, or integral length scale L in DNS calculations) and U is the main flow velocity. We intend to consider this two-scale motion with small parameter methods, mainly with the method of multiple scales. In the majority of published experiments, in the oceanic and atmospheric observations the inverse Froude number $F = NM/U$, representing the ratio of mass elevating forces to inertia forces, is rather small (of the order 10^{-2}). So, the equations describing turbulence evolution in stratified media contain the perfect small parameter $\varepsilon = F^2$ and can be effectively solved by means of small parameter decomposition. The use of a multiple scale method lets us obtain the equations describing short and long-time motion, combined by their internal link. The period and amplitude of internal wave motion together with the wave averaged behavior of the functions can be found in this way. The analytical study should explain some earlier detected laws, describing the dependence of a solution on Prandtl and Froude numbers and make conclusions about the rate and mechanism of stratified turbulence decay.

In the section we shall mainly concern ourselves with the parameters of wave motion. Subsequent sections will describe asymptotic regimes of short and long evolution time. Finally, we shall describe some features of turbulence evolution at not small Froude numbers, F, and the influence of the initial condition.

2. GOVERNING EQUATIONS

The evolution of grid-generated turbulence in uniform horizontal flow in the presence of vertical density gradient is considered. Before starting the description of the method it is necessary to say something about the nearly homogeneous turbulence model, we use the one described in ref. [1]. Nearly homogeneous turbulence is the simplest form of non-homogeneous turbulence driven by constant gradients of mean velocity and scalar field [15]. One of the attractive features of nearly homogeneous turbulence theory is that most of the existing experimental data refer to constant gradients [7–9, 16]. The second order closure

model [1], having been applied to homogeneous stratified flow [2], showed not a bad agreement with experiments in a salt-water tank [9] and in air wind tunnel [8].

In spite of a great importance of experimental and DNS methods for the understanding of physical phenomena in a stratified fluid, their application for long evolution time is rather hard. In view of the inevitable computing difficulties an application of DNS is now limited by Reynolds and molecular Prandtl numbers and short time intervals [17]. Experimental methods either do not give the possibility of studying the turbulence decay during very long time intervals, taking into account tiny magnitudes of values being measured and the necessity for having a very large experimental installation. The theory of nearly homogeneous turbulence can be a proper alternate method for very long time intervals, which is impossible for other methods of research.

In the theory of ref. [1] using the expression obtained for the two-point correlation $\overline{u_i u_j}$ and $\overline{u_i u_j u_k}$ it was shown that the Reynolds stress dissipation tensor can be parametrized in the form $\varepsilon_{ij} = \frac{1}{3}\varepsilon_u[dK_{ij} + (1-d)\delta_{ij}]$ where ε_u is the dissipation rate of TKE, $K_{ij} = \overline{u_i u_j}/\overline{u_i^2}$, the anisotropy coefficient, δ_{ij} the Kroneker symbol, and d is a certain normalized function of turbulence Reynolds number influence ($d = 0$ at $R_\lambda \gg 1$ and $d = 1$ at $R_\lambda \ll 1$). By comparing the above expression for ε_{ij} to the known Rotta's approximation [18] for the ε_{ij} tensor, $\varepsilon_{ij} = C_1 v/u_i u_j L^2 + C\overline{u_i^3}/L$, the parameter $d(R_\lambda)$ can be found in the form

$$d = 1 - 2/(1 + \sqrt{1 + \delta_u/R_\lambda^2})$$

where $\delta_u = 20C_1/C^2$ is some unknown constant. This constant was estimated to be equal to 2800 from Shuman and Petterson's work [19]. Other unknown terms of the model [1] were also parametrized using the $d(R_\lambda)$ function to satisfy limiting conditions of strong ($R_\lambda \gg 1$) and weak ($R_\lambda \ll 1$) turbulence.

The model of ref. [1] for uniform horizontal flow with constant vertical density gradient incorporates differential equations for doubled TKE, $\overline{u_i^2}$, intensity of scalar fluctuation, $\overline{\rho^2}$, vertical component of Reynolds tensor, $\overline{u_2 u_2}$, vertical mass flux, $\overline{\rho u_2}$, dissipation rates of TKE, ε_u, and of scalar fluctuation intensity, ε_ρ

$$\frac{1}{2}\frac{\mathrm{d}}{\mathrm{d}\tau^*}(\overline{u_2 u_2}) = -\left[\left(d + \frac{9}{2}(1-d)\right) \times \left(K - \frac{1}{3}\right) + \frac{1}{3}\right]\varepsilon_u - \frac{4}{5}b$$

$$\frac{1}{2}\frac{\mathrm{d}}{\mathrm{d}\tau^*}(\overline{u_i^2}) = -b - \varepsilon_u$$

$$\tau_u \frac{\mathrm{d}\varepsilon_u}{\mathrm{d}\tau^*} = F_u^{**}\varepsilon_u - 2\alpha_2 Rb \qquad (1)$$

$$\frac{\mathrm{d}}{\mathrm{d}\tau^*}(\overline{\rho u_2}) = \frac{\overline{\rho^2}\boldsymbol{g}}{\bar{\rho}}\left[d\left(K - \frac{1}{3}\right) - \frac{2}{3}\right] - \overline{u_2 u_2}\frac{\mathrm{d}\bar{\rho}}{\mathrm{d}x_2} - \left[(1-d) \times \left(\frac{1}{3} + 10KR\right) + \alpha_1 R\right]\overline{\rho u_2}\frac{\varepsilon_u}{\overline{u_i^2}}$$

$$\frac{1}{2}\frac{\mathrm{d}}{\mathrm{d}\tau^*}(\overline{\rho^2}) = -\overline{\rho u_2}\frac{\mathrm{d}\bar{\rho}}{\mathrm{d}x_2} - \varepsilon_\rho$$

$$\tau_\rho \frac{\mathrm{d}\varepsilon_\rho}{\mathrm{d}\tau^*} = -\left(\frac{F_{\rho 1}^{**}}{R} + F_{\rho 2}^{**}\right)\varepsilon_\rho + \frac{2\alpha_2}{\sigma}\left(-\overline{\rho u_2}\frac{\mathrm{d}\bar{\rho}}{\mathrm{d}x_2}\right)$$

where F_u^{**}, $F_{\rho 1}^{**}$, $F_{\rho 2}^{**}$ * are the interaction functions of the turbulent vortices of different scales for the isotropic velocity and scalar fields parametrized in ref. [1] as

$$F_u^{**} = \tfrac{11}{3} - \tfrac{13}{15}d, \quad F_{\rho 1}^{**} = \tfrac{5}{3}(1-d), \quad F_{\rho 2}^{**} = 2 + \tfrac{4}{3}d,$$

$b = (\overline{\rho u_2}/\bar{\rho})\boldsymbol{g}$ is the buoyancy vector (positive if upward), $K = \overline{u_2 u_2}/\overline{u_i^2}$ is the vertical anisotropy coefficient, $\tau_u = \overline{u_i^2}/\varepsilon_u$ the velocity field time scale, $\tau_\rho = \overline{\rho^2}/\varepsilon_\rho$ the scalar field time scale, $R = \tau_u/\tau_\rho$ the time scale ratio, $\alpha_1 = 2d(\sigma_\infty + 3/5)/R_\infty$, $\alpha_2 = \alpha_1\sigma/(1+\sigma)$ are coefficients dependent on d and σ, σ_∞ and R_∞ are the asymptotic values of turbulent Prandtl and of time scale ratio in passive scalar case ($F = 0$) at $\tau \to \infty$ taken from the work in ref. [20]

$$\sigma_\infty = \frac{3(1-\sigma)}{10\sigma}\left[1 - \left(\frac{2\sigma}{1+\sigma}\right)^{3/2}\right]^{-1} \qquad (2)$$

$$R_\infty = \frac{1}{5\sigma}\left[1 - \left(\frac{2\sigma}{1+\sigma}\right)^{3/2} + \sigma^{3/2}\right] \times \left[1 - 2\left(\frac{2\sigma}{1+\sigma}\right)^{1/2} + \sigma^{1/2}\right]^{-1}. \qquad (3)$$

In dimensionless form the system being analyzed takes the form

$$\frac{\mathrm{d}R_{22}}{\mathrm{d}\tau} = -2\left\{\frac{1}{3}\left[d + \frac{9}{2}(1-d)\right]\left(3\frac{R_{22}}{E} - 1\right) + \frac{1}{3} + \frac{4}{5}Q\frac{T_u}{E}F^2\right\}\frac{E}{T_u}$$

$$\frac{\mathrm{d}E}{\mathrm{d}\tau} = -2\left[1 + Q\frac{T_u}{E}F^2\right]\frac{E}{T_u}$$

$$\frac{\mathrm{d}T_u}{\mathrm{d}\tau} = (F_u^{**} - 2) - 2\left[1 - d\left(\frac{2\sigma}{1+\sigma}\right)\left(\sigma_\infty + \frac{3}{5}\right)\frac{1}{R_\infty}\frac{T_u}{T_\rho}\right]F^2\frac{QT_u}{E}$$

$$\frac{\mathrm{d}Q}{\mathrm{d}\tau} = -F^2\left[\frac{2}{3} - \frac{1}{F^2}\frac{R_{22}}{\Theta} - d\left(\frac{R_{22}}{E} - \frac{1}{3}\right)\right]\Theta$$

$$-\left[(1-d)\left(\frac{1}{3}+10\frac{R_{22}T_u}{ET_\rho}\right)\right.$$

$$\left.+2d\left(\sigma_\infty+\frac{3}{5}\right)\frac{1}{R_\infty}\frac{T_u}{T_\rho}\right]\frac{Q}{T_u}$$

$$\frac{d\Theta}{d\tau}=-2\left[1-Q\frac{T_\rho}{\Theta}\right]\frac{\Theta}{T_\rho}$$

$$\frac{dT_\rho}{d\tau}=(F_{\rho 2}^{**}-2)+F_{\rho 1}^{**}\frac{T_\rho}{T_u}$$

$$-d\frac{4}{3}\left(1-\frac{3}{5R_\infty}\right). \tag{4}$$

3. THE CHOICE OF EXPANSION METHOD

Using a small parameter method we should expand the functions in system (1) in power series of ε, combining the terms with identical exponents ε in separate subsystems. It is valid if the identical order of magnitude in subsystems is not infringed by any other factors. In our case, we have to mention some of such factors in system (1). The time scales T_u and T_ρ grow near-linearly with τ, for a strong turbulence mode ($R_\lambda \gg 1$) the parameter d tends to zero; oppositely for a weak turbulence mode, the parameter $d' = 1-d$ tends to zero. So, it is hardly possible to obtain an approximate solution uniformly valid for all τ and R_λ. A set of partial cases will be considered instead.

A direct expansion on a small parameter ε in (1) is singular for $\tau > 1$ in asymptotic expansions sense [21], because it contains positive exponents of τ enlarging with the order of approach. Mathematically, this singularity is caused by differential order lowering in equation (1), as at $\tau \gg 1$ the differential equation for the turbulent mass flow degenerates into an algebraic form. To obtain an asymptotic expansion, valid at long τ, it is necessary to replace the variables, using for this purpose the small parameter ε in new variables.

Existing information indicates from which class of functions an approximate solution should be constructed. The results of ref. [2] (and of many works mentioned in the Introduction) showed that the functions in equation (1) can be represented as monotonous dependencies with oscillations imposed. Proceeding from the published numerical solutions we shall seek an approximate analytical solution for any of the functions f in equation (1) as a sum of harmonic function with varying amplitude $\tilde{f}$ and some smooth additive $\hat{f}$, i.e. $f=\hat{f}+\tilde{f}=\hat{f}+\tilde{f}'\tilde{f}''$, where $\tilde{f}'$ is the amplitude and $\tilde{f}''$ is the harmonic function.

We shall further subdivide our analysis into three time spans, near, distant and final. Generally, the most important is the distant time span, which can be defined by the condition $T_\rho \gg 1$. The near time interval ($T_\rho \sim 1$) is rather small and generally speaking is absent if initial conditions determine a large size of T_ρ (practically $T_\rho > 10$). The final time span is a partial and more simple case of the distant one. We shall consider asymptotic modes of near and final time spans in the next sections of this paper.

4. ANALYSIS OF DISTANT TIME SPAN

Let us introduce the following set of variables and coordinates

$$q=\varepsilon T_\rho Q/E,\quad \vartheta=\varepsilon\Theta/E,\quad K=R_{22}/E,$$
$$R=T_u/T_\rho,\quad t=\varepsilon T_\rho,\quad \tilde{\tau}=e\tau=N\tau^*$$

where $e=\varepsilon^{1/2}=F$, T_u and T_ρ are non-dimensional time scales for velocity and scalar fields, ϑ represents the relation of potential energy $\varepsilon\Theta$ to the kinetic energy E, the functions t and $\tilde{\tau}=N\tau^*$ are used further as independent variables. In these designations the original system of equations (4) can be written more briefly as

$$t\frac{dK}{d\tau}=\varepsilon\frac{-7d'(K-1/3)}{R}+2\varepsilon q(K-4/5)$$

$$t\frac{dR}{d\tau}=\varepsilon\frac{4}{5}d(1-R/R_\infty)-2\varepsilon q(1-\alpha_2 R)R$$

$$t\frac{d\vartheta}{d\tau}=2\varepsilon\left(\frac{1}{R}-1\right)\vartheta+2\varepsilon q(1+\vartheta)$$

$$t\frac{dq}{d\tau}=t^2A_1+\varepsilon q\left[\frac{1}{R}\left(2-\frac{d'}{3}\right)-10d'K-\alpha_1+p\right]+2\varepsilon q^2$$

$$\frac{dt}{d\tau}=\varepsilon p$$

$$t\frac{dE}{d\tau}=-\frac{2\varepsilon E}{R}-2\varepsilon qE \tag{5}$$

where $p=4d/5R_\infty+5d'/3R$ and

$$A_1=K+\vartheta[d(K-1/3)-2/3]. \tag{6}$$

At $d=$ const. (at asymptotically large $R_\lambda \gg 1$ and small $R_\lambda \ll 1$ turbulent Reynolds numbers) the equation for E in equation (5) can be solved separately from the other equations. At turbulent Reynolds numbers, not satisfying these two extreme cases it is more convenient to replace the equation for E in equation (5) with the equation for d, which is the equation for the turbulent Reynolds number, R_λ, and can be deduced from equations for E and T_u in equation (5) as

$$t\frac{d(d)}{d\tau}=\varepsilon p_1\left(\frac{F_u^{**}-4}{R}-2(2-\alpha_2 R)q\right) \tag{7}$$

where p_1 is a logarithmic derivative of d with respect to R_λ^2. Its calculation gives

$$p_1=\frac{d(d)}{d(R_\lambda^2)}R_\lambda^2=(1/(1+\delta_u/R_\lambda^2)^{1/2}-1)$$
$$\times(1+(1+\delta_u/R_\lambda^2)^{1/2})^{-1}=-\frac{dd'}{(1+d)}.$$

The density field time scale function, $T_\rho(\tau)$, grows monotonously with τ and can be used as an independent variable, replacing τ in equations (5) and (7). We shall, however, use the independent variable T_ρ instead of τ, but alongside with τ (strictly speaking, alongside with $\tilde{\tau}$), applying a known method of multiple scales [21], which expands the derivatives. We shall seek the desired functions in the following form

$$\begin{aligned} K &= \hat{K}(t)+\varepsilon\tilde{K}(t,\tilde{\tau})+O(\varepsilon^2),\\ R &= \hat{R}(t)+\varepsilon\tilde{R}(t,\tilde{\tau})+O(\varepsilon^2)\\ \vartheta &= \hat{\vartheta}(t)+\varepsilon\tilde{\vartheta}(t,\tilde{\tau})+O(\varepsilon^2),\\ d &= \hat{d}(t)+\varepsilon\tilde{d}(t,\tilde{\tau})+O(\varepsilon^2)\\ q &= \hat{q}(t)+e\tilde{q}(t,\tilde{\tau})+O(e^2). \end{aligned} \tag{8}$$

The decomposition of all the functions in equation (8), except q, is carried out on ε, but with q on $e=\sqrt{\varepsilon}$. The use of an alternate method of matched asymptotic expansions (MAE) could explain the presence of the different exponents of ε in expansions for q and for the other functions in equation (8). Let us describe briefly the scheme of the MAE method in our case.

According to the MAE method the general solution can be constructed in a kind of a sum of inner and outer solutions minus their conterminous part [22]. The outer solutions in our case are the functions 'with a cover'. The inner solution is performed with the 'stretched' variable $\tilde{\tau}=\tau/e$. In the first approach (on e) of internal expansion the simple solution is obtained: q is a harmonic function, and the rest of the functions are constant, which, as follows from an asymptotic matching principle, are equal to the outer solutions for the appropriate functions. Substituting them into the second order approach system of internal expansion we can find oscillations of the other functions; they will be multiplied by $\varepsilon=e^2$ in resulting solution. On the contrary, oscillations in the internal solution for q will be multiplied by e.

Substituting expansions (8) into system (5) and gathering the terms with identical exponents of ε we obtain two systems. One of them, for the functions with a cover, equation (9), has the form

$$\begin{aligned} pt\frac{\mathrm{d}\hat{K}}{\mathrm{d}t} &= -7\frac{\hat{d}'(\hat{K}-1/3)}{\hat{R}}+2\hat{q}(\hat{K}-4/5)\\ tp\frac{\mathrm{d}\hat{R}}{\mathrm{d}t} &= \frac{4}{5}\hat{d}(1-\hat{R}/R_\infty)-2(1-\alpha_2\hat{R})\hat{R}\hat{q}\\ 0 &= t^2\hat{A}_1,\\ tp\frac{\mathrm{d}\hat{\vartheta}}{\mathrm{d}t} &= 2\left(\frac{1}{\hat{R}}-1\right)\hat{\vartheta}+2\hat{q}(1+\hat{\vartheta})\\ tp\frac{\mathrm{d}(\hat{d})}{\mathrm{d}t} &= p_1\left[\frac{F_u^{**}-4}{\hat{R}}-2(2-\alpha_2\hat{R})\hat{q}\right]\\ tp\frac{\mathrm{d}\hat{E}}{\mathrm{d}t} &= -\frac{2\hat{E}}{\hat{R}}-2\hat{q}\hat{E} \end{aligned} \tag{9}$$

where the functions α_1, α_2, $\hat{A}_1$, p_1 and F_u^{**} depend on the functions with a cover, too. The oscillations in equation (5) are described by the following system

$$\begin{aligned} t\frac{\partial\tilde{K}}{\partial\tilde{\tau}} &= 2\tilde{q}(\hat{K}-4/5)\\ t\frac{\partial\tilde{R}}{\partial\tilde{\tau}} &= -2\tilde{q}(1-\alpha_2\hat{R})\hat{R}\\ t\frac{\partial\tilde{q}}{\partial\tilde{\tau}} &= t^2\tilde{A}_1+f(t)\\ t\frac{\partial\tilde{\vartheta}}{\partial\tilde{\tau}} &= 2\tilde{q}(1+\hat{\vartheta})\\ t\frac{\partial(\tilde{d})}{\partial\tilde{\tau}} &= -2p_1\tilde{q}(2-\alpha_2\hat{R})\\ t\frac{\partial\tilde{E}}{\partial\tilde{\tau}} &= -2\tilde{q}\hat{E} \end{aligned} \tag{10}$$

where

$$f(t) = -t\frac{\mathrm{d}\hat{q}}{\mathrm{d}t}+\hat{q}\left[\hat{R}^{-1}\left(2-\frac{\hat{d}'}{3}\right)-10\hat{d}'\hat{K}-\alpha_1+p\right]+2\hat{q}^2 \tag{11}$$

and $\tilde{A}_1$ presents the second term in the expansion for A_1:

$$A_1 = \hat{A}_1(\hat{K},\hat{\vartheta},\hat{d})+\varepsilon\tilde{A}_1. \tag{12}$$

The equation for $\tilde{q}$ is obtained from the expansion terms with the exponent εe in the fourth line of equation (5).

$$tp\frac{\partial\tilde{q}}{\partial t} = \tilde{q}\left[\hat{R}^{-1}\left(2-\frac{\hat{d}'}{3}\right)-10\hat{d}'\hat{K}-\alpha_1+p\right]+4\tilde{q}\hat{q}. \tag{13}$$

The differential equation for $\hat{q}$ degenerates into an algebraic form in system (9). The value of the variable t is not small, whence $\hat{A}_1=0$. This expression is an approximate integral of system (5). Differentiating this relation with respect to t, we obtain another approximate integral,

$$pt\frac{\mathrm{d}\hat{A}_1}{\mathrm{d}t} = 2(c_1+c_2\hat{q}) = 0 \tag{14}$$

where

$$\begin{aligned} c_1 &= -\frac{7}{2}(1+\hat{\vartheta}\hat{d})\hat{d}'(\hat{K}-1/3)\hat{R}^{-1}+\hat{\vartheta}[\hat{d}(\hat{K}-1/3)\\ &\quad -2/3](\hat{R}^{-1}-1)+\hat{\vartheta}(\hat{K}-1/3)\frac{p_1}{2}(F_u^{**}-4)\hat{R}^{-1}.\\ c_2 &= (1+\hat{\vartheta}\hat{d})(\hat{K}-4/5)+[\hat{d}(\hat{K}-1/3)-2/3]\\ &\quad (1+\hat{\vartheta})+\hat{\vartheta}(\hat{K}-1/3)p_1(2-\alpha_2\hat{R}). \end{aligned}$$

Expressing $\hat{q}$ from equation (14), we get

$$\hat{q} = -c_1/c_2. \tag{15}$$

The relation (15) should replace the fourth line of system (9) for the smooth components. In this case the third line of system (9) is used for the determination of $\hat{\vartheta}$. All other lines of system (9) coincides with systems (5) and (7).

Consider now the solution of system (10). Differentiating partially the third equation of (10) with respect to $\tilde{\tau}$, yields

$$\frac{\partial^2 \tilde{q}}{\partial \tilde{\tau}^2} = t\frac{\partial \tilde{A}_1}{\partial \tilde{\tau}}. \tag{16}$$

The differential equation for the function A_1 can be deduced by the differentiation of equation (6) with respect to τ. It has the form

$$t\frac{dA_1}{d\tau} = 2(c_1 + c_2 q). \tag{17}$$

Applying the expansion on the powers of e, equation (12), in this equation we obtain the following relation for the wave component of A_1-function.

$$t\frac{\partial \tilde{A}_1}{\partial \tilde{\tau}} = 2c_2\tilde{q}. \tag{18}$$

The analysis shows, that c_2 is negative. Denoting

$$\omega^2 = -2c_2 \tag{19}$$

we write a wave equation for $\tilde{q}$

$$\frac{\partial^2 \tilde{q}}{\partial \tilde{\tau}^2} + \omega^2\tilde{q} = 0. \tag{20}$$

The solution of equation (20) is a harmonic function of $\tilde{\tau}$ multiplied by an arbitrary function of t. Separating the variables with $\tilde{q} = \tilde{q}'(t)\tilde{q}''(\tilde{\tau})$, we obtain

$$q'' = \sin(\omega\tau + \varphi_0).$$

Substituting then the expression for $\tilde{q}$: $\tilde{q} = \tilde{q}'(t)\sin(\omega\tilde{\tau} + \varphi_0)$ into system (11), we can find out other wave components. For the function $\tilde{K}$, for example, it gives

$$\tilde{K} = \tilde{K}'\tilde{K}'' = -2\frac{\tilde{q}'(\hat{K} - 4/5)}{t\omega}\cos(\omega\tilde{\tau} + \phi_0)$$

so we conclude

$$\tilde{K}' = -2\frac{\tilde{q}'(\hat{K} - 4/5)}{t\omega}, \quad \tilde{K}'' = \cos(\omega\tilde{\tau} + \phi_0). \tag{21}$$

Similarly the amplitudes and phases of other wave component can be found

$$\tilde{R}' = 2\frac{\tilde{q}'(1 - \alpha_2\hat{R})\hat{R}}{t\omega}, \quad \tilde{R}'' = \cos(\omega\tilde{\tau} + \phi_0) \tag{22}$$

$$\tilde{\vartheta}' = -2\frac{\tilde{q}'(1 + \hat{\vartheta})}{t\omega}, \quad \tilde{K}'' = \cos(\omega\tilde{\tau} + \phi_0) \tag{23}$$

$$\tilde{d}' = 2p_1\frac{\tilde{q}'(2 - \alpha_2\hat{R})}{t\omega}, \quad \tilde{d}'' = \cos(\omega\tilde{\tau} + \phi_0) \tag{24}$$

$$\tilde{E}' = 2\frac{\tilde{q}'\hat{E}}{t\omega}, \quad \tilde{E}'' = \cos(\omega\tilde{\tau} + \phi_0). \tag{25}$$

It follows from equations (21)–(25), that amplitudes of all functions are proportional to the amplitude of the mass flow oscillation that all functions oscillate with the same frequency, and that the phases of oscillations for $\tilde{K}$, $\tilde{R}$, $\tilde{\vartheta}$, $\tilde{d}$, $\tilde{E}$ are shifted to a quarter of a period from the phase of $\tilde{q}$. At long t the oscillations of all functions, besides q, are small. Exactly the same behavior of the functions is pointed out in the numerical results.

The oscillations of functions in equation (10) are generated by the oscillation of the cross turbulent mass flux, $\tilde{q}$. At the same time, the oscillation of the flux is caused by the oscillation of function A_1, see equation (18). The varying which occurs under the cosine law function $\tilde{A}_1$ may be referred to as amplitude one, since all the amplitudes are proportional to $\tilde{A}_1$. An appropriate second order differential equation for $\tilde{A}_1$ can be obtained differentiating equation (18) with respect to $\tilde{\tau}$

$$\frac{\partial^2 \tilde{A}_1}{\partial \tilde{\tau}^2} + \omega^2\tilde{A}_1 = -\omega^2\frac{f(t)}{t^2}$$

whence the dependence $\tilde{A}_1$ on $\tilde{\tau}$ and t can be written in the form

$$\tilde{A}_1 = -f(t)/t^2 + \tilde{A}_1'\cos(\omega\tilde{\tau} + \phi_0)$$

where $\tilde{A}_1'$ is a function dependent on t only; different to the other functions with tilde, function $\tilde{A}_1$ has a non-zero additive component, $-f(t)/t^2$. Since $\hat{A}_1 = 0$, at long evolution time t this component represents a very small wave-averaged value of A_1, related to which oscillations take place. The amplitude of oscillation $\tilde{q}'$ is connected to the amplitude of oscillation $\tilde{A}_1'$ by the relation

$$q' = \tilde{A}_1' t/\omega. \tag{26}$$

Presenting $\tilde{q}$ in equation (13) in the form of a product $\tilde{q} = \tilde{q}'(t)\tilde{q}''(\tilde{\tau})$ we find out an exponent in the power law for $\tilde{q}'(t)$ from the ordinary differential equation

$$\frac{t}{\tilde{q}'}\frac{d\tilde{q}'}{dt} = p^{-1}\left[\frac{1}{\hat{R}}\left(2 - \frac{\hat{d}'}{3}\right) - 10\hat{d}'\hat{K} - \alpha_1 + p + 4\hat{q}\right]. \tag{27}$$

At $t \to \infty$ the r.h.s. of equation (27) tends to a constant value. It determines a power law for the amplitude $\tilde{q}'$ and, hence, for all other amplitudes. It will be considered in more detail at the analysis of the final stage of decay in the next part of this paper.

For testing the relations obtained above it is necessary to solve numerically the full system of equations (5)–(7) and the system for the functions 'with a cover' equations (9) and (15). Preliminarily, in order to more

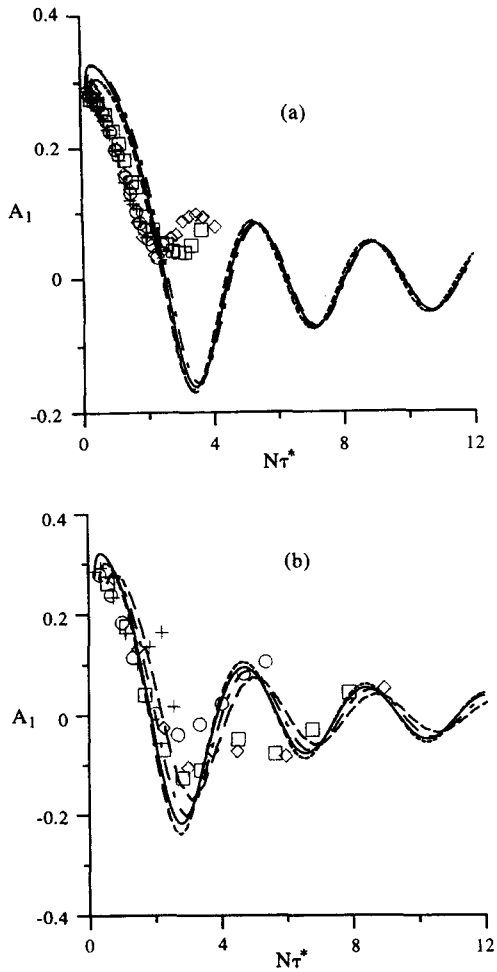

Fig. 1. The variation of function A_1 in the experiment (symbols) and in the calculations (lines): (a) in conditions of ref. [8] for air (◇) $F = 0.0492$, (□) $F = 0.0441$, (○) $F = 0.0302$, (+) $F = 0.0236$; (b) in conditions of ref. [9] for water (◇) $F = 0.149$, (□) $F = 0.113$, (○) $F = 0.067$, (+) $F = 0.036$.

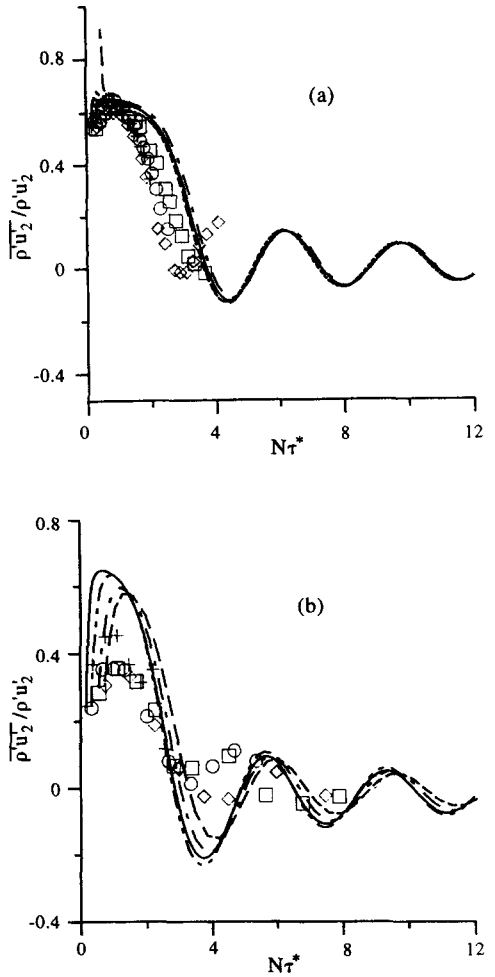

Fig. 2. The variation of vertical convective correlation coefficient $\overline{\rho' u_2'}/\rho' u_2'$ in the experiment (symbols) and in the calculations (lines): (a) in conditions of ref. [8] for air; (b) in conditions of ref. [9] for water. For symbols, see Fig. 1.

definitely recommend the model itself [1] to practical use we made comparisons with the experiments of refs. [9] and [8] in addition to published ones, [2]. Other experimental points (first points in each experimental set instead of third or fourth points in ref. [2]) were chosen as the initial conditions for calculation and some other functions were compared.

Figure 1 plots the function $A_1(\tau)$. In both the cases $\sigma = 0.73$ (Fig. 1(a)) and $\sigma = 800$ (Fig. 1(b)) there is a close agreement between the model and the experiments. Function $A_1(\tau)$ oscillates with the same frequency, the wave averaged value $\hat{A}_1$ being really small and tending to zero. Figure 2 shows vertical convective flux correlation coefficient. In accordance with the model the phases of oscillations here and in the previous sketch are noticeably shifted. The duration of the first period in calculation was probably higher than in the experiment due to aperiodic disturbance produced by the initial conditions. This disturbance can be practically avoided by starting the calculation from subsequent experimental points. Nevertheless, the degree of compatibility is rather good. Unfortunately, there are no experimental points for $N\tau^* > 4$ in the air case. The variation of TKE in the calculation looks like that observed in experiments (Fig. 3). For the function $\Gamma = g/\bar{\rho}(\varepsilon_\rho/\varepsilon_u d\bar{\rho}/dx_2) = \theta R$, representing a mixing efficiency in the ocean, [6], predicted and experimental values are initially close, but after the onset of collapse some experimental points disagree (Fig. 4). It should be noted that for these points the inverse Froude number is not small enough.

The comparison of the numerical solution of the two systems (5)–(7) and (9), (15) shows, that the second system really describes the averaged oscillation behavior of the first system with a very high accuracy. The subsequent parts of the paper contain detailed results of such a comparison for near and final time spans.

Calculated according to equation (19) the period of oscillation, $T = 2\pi/\omega$, coincides with the results of ref. [2] completely within the limits of such comparison accuracy (Fig. 5(a)). Here, and below initial conditions for the comparison with ref. [2] were taken

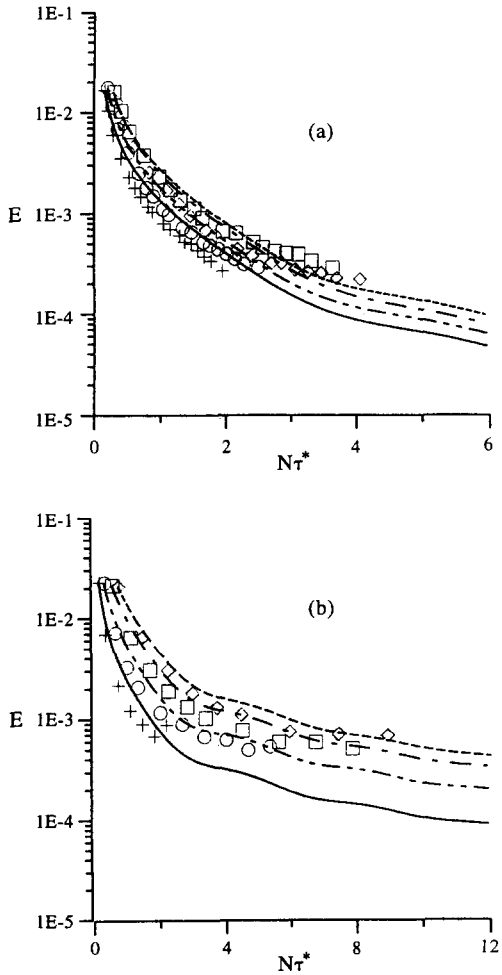

Fig. 3. The variation of turbulence kinetic energy E in the experiment (symbols) and in the calculations (lines): (a) in conditions of ref. [8] for air; (b) in conditions of ref. [9] for water. For symbols, see Fig. 1.

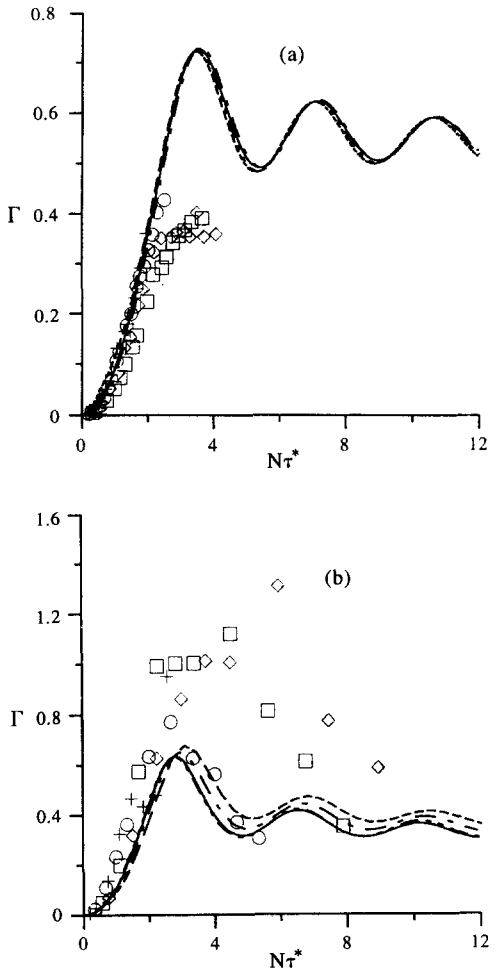

Fig. 4. The variation of mixing efficiency Γ in the experiment (symbols) and in the calculations (lines): (a) in conditions of ref. [8] for air; (b) in conditions of ref. [9] for water. For symbols, see Fig. 1.

from the experimental points of ref. [8] (Table 4, $N = 1.16, x/M = 11.9$) in the air case ($\sigma = 0.73$, $F = 2.4 \times 10^{-2}$, $M = 5.08 \times 10^{-2}$, $Re = 7900$) and of ref. [9] (Table 2b, $N = 0.24, x/M = 30$) in the water case ($\sigma = 800, F = 3.7 \times 10^{-2}, M = 3.81 \times 10^{-2}$, $Re = 9500$). It is to be noted, that the cases of water with $\sigma = 800$ and air with $\sigma = 0.73$ correspond to different values of this period at $t \to \infty$. It causes the difference of the K-value for these two cases. Oppositely, there is a small distinction of these two cases at $t \sim 1$.

The oscillating behavior of the variation of vertical mass flux together with the fast decay of the amplitude $\tilde{q}'$ was earlier pointed out in a recent DNS of the problem made in ref. [10]. The period of the flux oscillation (see also ref. [17]) was found to be approximately equal to one half of the Brunt–Väisälä period. It agrees well with the current results (see Fig. 2). To compare the period of oscillations more definitely we also plot (calculated according to formula (19)) predicted and experimental values of $T = 2\pi/\omega$. As follows from the analysis made above, the period of oscillations depends on wave averaged functions, but in Fig. 6 we compare the predicted values of period with non averaged experimental points. In spite of this, the agreement looks rather good for air and for water (Fig. 6).

The next step of testing is a comparison of oscillating components in numerical solutions with analytical predictions. For this purpose the numerical solution of system (9), (15) should be subtracted from the numerical solution of system (5)–(7) for appropriate functions. The results for the differences $f_i - \hat{f}_i$ where $i = K, R, q_1, \vartheta, E, d, A_1$ and $q_1 = q/\varepsilon$ are shown in Fig. 7(a). To extract the wave components more precisely one has to adjust the initial conditions for the functions 'with a cover', which differ from the initial conditions for system (5)–(7). After such adjusting, the wave components look more informative (Fig. 7(b)). The oscillating components represented in Fig. 7(b) correspond to the following differences $\hat{f} - f$ at the initial point: $\hat{K} - K = 9.0 \times 10^{-3}$, $\hat{R} - R = 1.0 \times 10^{-1}$, $\hat{\vartheta} - \vartheta = 0.162$, $\hat{E} - E = -2.7 \times 10^{-4}$, $\hat{d} - d = 1.29 \times 10^{-2}$.

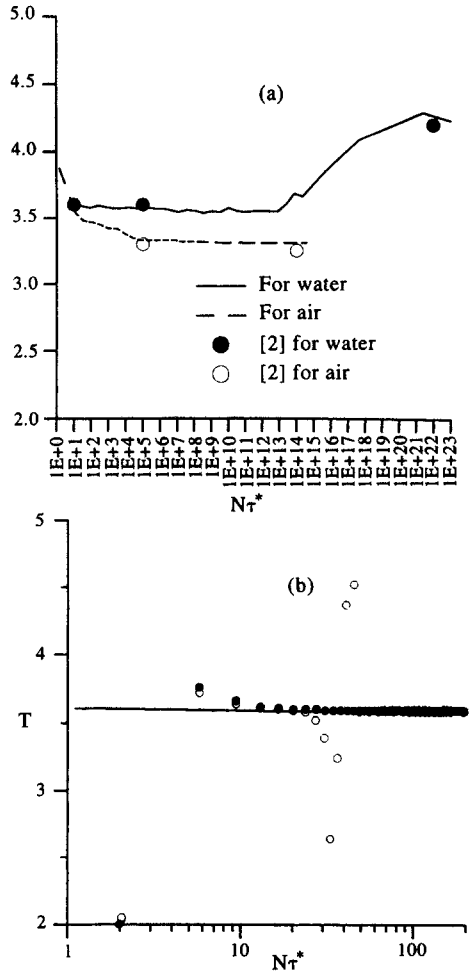

Fig. 5. Comparison of analytically predicted according to equation (19) (lines) and the numerically obtained (symbols) period of oscillation: (a) comparison with the results of ref. [2] for a large time span; (b) comparison with our own numerical calculation for initial time span (hollow circles—period for R-function; filled circles—period for K, ϑ, E, d).

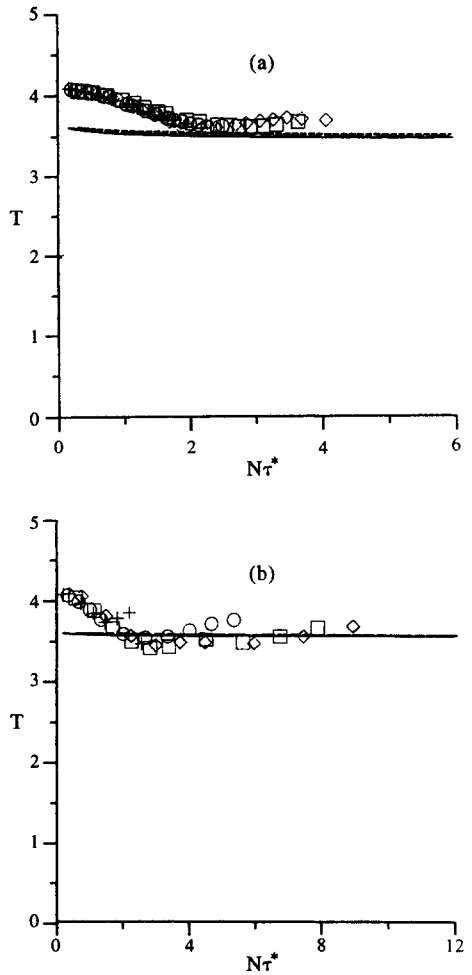

Fig. 6. The variation of oscillation period, T in the experiment (symbols) and in the calculations (lines): (a) in conditions of ref. [8] for air; (b) in conditions of ref. [9] for water. For symbols, see Fig. 1.

The phases of oscillations of E and ϑ are opposite (Fig. 7(b)). A reduction of one of them causes an increase of the other one. The oscillations of K are in phase with the oscillations of E, but are more sharp. The same picture was observed in numerical calculations of ref. [2] and in a number of works based on the DNS application (see ref. [17]).

There are two positions in which the wave component of the turbulent mass flux, $\tilde{q}$, is equal to zero, we shall name them A and B. In position A the functions $\tilde{\vartheta}$, $\tilde{R}$, $\tilde{d}$ have a maximum and $\tilde{E}$, $\tilde{K}$ and $\tilde{A}_1$ have a minimum, sign of convective mass flux reverts from plus (upwards) to minus (downwards). This situation occurs after lifting up of more easy turbulent patches and corresponds to a more significant density stratification, as it follows from the N number. In position A velocity fluctuations are partially extinguished. In position B the wave component of mass flux, $\tilde{q}$, changes the sign from negative to positive. After lowering down more easy turbulent patches the density field becomes more uniform, the density fluctuations are extinguished, while the velocity fluctuations grow.

Having extracted the oscillations, it is possible then to analyze their amplitudes. Figure 8 compares the amplitudes taken from the numerical solution of the full system (5) with the amplitudes calculated from smoothed system (9), (15) together with equations (27) and (21)–(26). Extracting the small oscillating components can lead to some loss of accuracy. We see, for instance, that the amplitude for $\tilde{d}$ (which is especially small) begins to differ from their predictions after a while (Fig. 8a). To extract the wave components more precisely it is necessary to adjust the initial conditions for $\hat{f}$ more accurately. Taking this into account the agreement in Fig. 8 appears satisfactory for all the functions besides R. The large difference between the analytically predicted and numerically calculated amplitude of the $\tilde{R}$-function near the axial coordinate $\tilde{\tau} = 20$ is caused by one principal reason. Just near this position the sign of

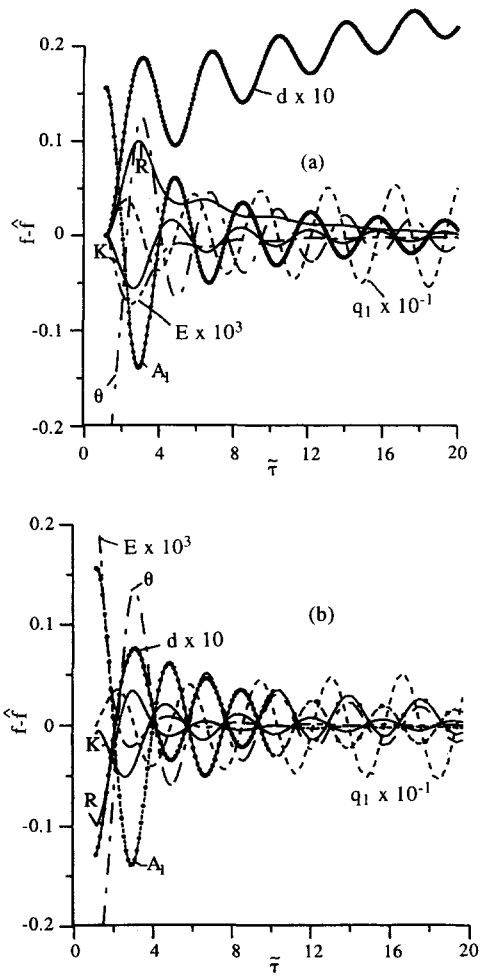

Fig. 7. Wave components $f_i - \hat{f}_i$ for the functions of the model: (a) before and (b) after, adjusting the initial conditions for smooth components $\hat{f}_i$.

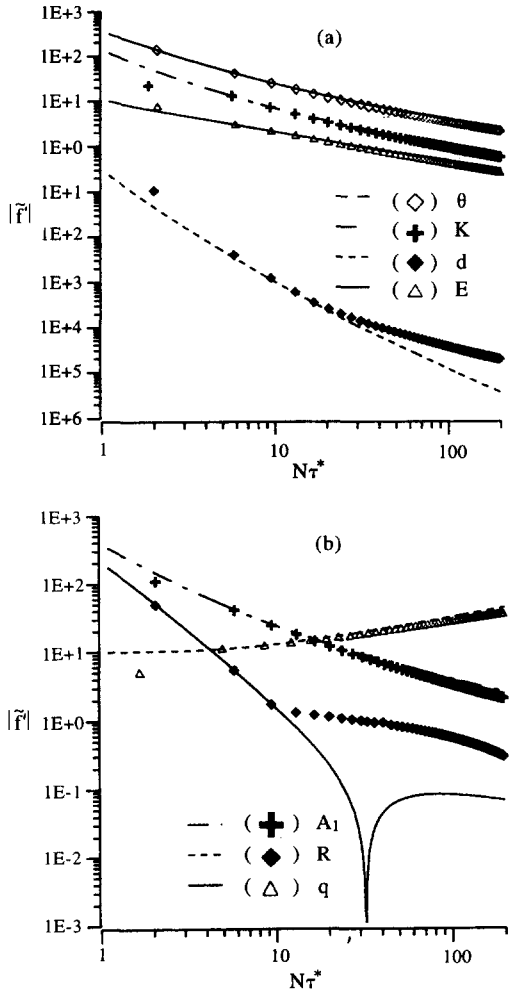

Fig. 8. Comparison of analytically predicted and numerically obtained amplitudes for the various functions of the model. Lines—predicted according to equations (21)–(26), symbols—numerical: (a) for $\tilde{\vartheta}'$, $\tilde{K}'$, $\tilde{d}'$, $\tilde{E}'$; (b) for $\tilde{A}_1'$, $\tilde{R}'$, $\tilde{q}'$.

$\tilde{R}'$ in equation (22), is changed, so we can discuss phenomenon of internal wave overturning. It is clear that near the point of zero $\tilde{R}'$ the procedure of asymptotic expansion applied in this section fails and should be corrected to include dispersion into consideration.

This can be proven to be true, by comparison of oscillation periods for the various functions with their analytical predicted (by equation (19)) values. As it is easy to see, periods of oscillations for all functions except R coincide with each other everywhere, but periods for R begin to differ from others near the point of zero $\hat{R}'$, Fig. 5(b). This phenomenon appears to be important because it can create other wave harmonics in the stream and must be related with increasing dissipation. Finally, we should note that original system (5) is stiff, so it is hard to solve it correctly over long time intervals. At the same time system (9) is not stiff and is much more convenient for calculations at very long time intervals.

5. CONCLUSIONS

For small inverse Froude numbers $F = NM/U$ the detailed analysis was made of the model in refs. [1, 2], describing an evolution of homogeneous turbulence in stably stratified media. The difference in time scales permits one to carry the mathematical separation of buoyancy and viscous dissipation processes. The infinitesimal of $\varepsilon = F^2$ is used to construct approximate analytical solutions. It is quite allowable for the practically important cases of density stratification in salt sea-water and temperature stratification in atmospheric air ($\varepsilon \sim 10^{-3}$).

Applying a small parameter method in the form of equation (8) to the original system of equations (5), it manages to separate the problem into the systems of equations (9), (15) for wave averaged functions, and system (10) for oscillating components. The form of the method used is rather common and can be repeated in other models describing the same or similar problem.

Due to intensive mixing behind the grid, turbulent patches appear in flow regions with different density. At small inverse Froude numbers the resulting force acting on them linearly depends on the displacement

of the patch from the equilibrium state. The equilibrium shown is defined by the relation $\hat{A}_1 = 0$ and relation (15) for the wave averaged convective flux $\hat{q}$. The expression $\hat{A}_1 = 0$ sets a mutual balance of squared density and vertical velocity fluctuations.

The presence of returning force proportional to the displacement leads to arising of harmonic oscillation. The function $A_1(\tau) = \hat{A}_1(t) + \varepsilon\tilde{A}_1(\tilde{\tau}, t)$ oscillates about its average nearly zero value. Oscillations of A_1 initiate oscillations of the turbulent vertical mass flux, shifted in phase on $\pi/2$. It forces all other functions in equation (5) to oscillate with the same frequency.

The variance of oscillation amplitude $\tilde{q}'$ is described by the differential equation (27). Amplitudes of the other functions and their places are related to the amplitude and the phase of q-fluctuations by the algebraic formulas (21)–(26). For the oscillating component of vertical mass flux, $\tilde{q}$, the wave equation (20) is deduced. The frequency of oscillations in equation (20) varies in accordance to relation (19).

The value of the mean flux $\hat{q}$ is rather small compared to the peak value of mass flux oscillation, but it can form a radical difference from an isotropic media case during long interval.

Acknowledgement—This work was supported, in part, by Soros Humanitarian Foundation Grant awarded by The American Physical Society.

REFERENCES

1. Kolovandin, B. A. Modelling the dynamics of turbulent transport processes. In *Advances in Heat Transfer*, 1991, Vol. 21. Academic Press, New York, pp. 185–234.
2. Kolovandin, B. A., Bondarchuk, V. U., Meola, C. and De Felice, G., Modelling of the homogeneous turbulence dynamics in stably stratified media. *International Journal of Heat and Mass Transfer*, 1993, **36,** 1953–1968.
3. Gibson, C. H., In *Marine Turbulence*, ed. J. Nihoul. Elsevier, Amsterdam 1980, pp. 221–257.
4. Dickey, T. D. and Mellor, G. L., Decaying in neutral and stratified fluid. *Journal of Fluid Mechanics*, 1980, **99,** 13–31.
5. Stillinger, D. C., Helland, K. N. and Van Atta, C. W., Experiments on the transition of homogeneous turbulence to internal waves in a stratified fluid. *Journal of Fluid Mechanics*, 1983, **131,** 91–122.
6. Hopfinger, E. J., Turbulence in stratified fluids. A review. *Journal of Geophysical Research*, 1987, **92,** 5287–5303.
7. Thorpe, S. A., Experiment of stability and turbulence in a stratified flow. *Journal of Fluid Mechanics*, 1973, **61,** 731–751.
8. Lienhard, J. H. and Van Atta, C. W., The decay of turbulence in thermally stratified flow. *Journal of Fluid Mechanics*, 1990, **210,** 57–112.
9. Itswiere, E. C., Helland, K. N. and Van Atta, C. W., The evolution of grid-generated turbulence in a stably stratified fluid. *Journal of Fluid Mechanics*, 1986, **162,** 229–338.
10. Yoon, K. and Warhaft, Z., The evolution of grid-generated turbulence under conditions of stable thermal stratification. *Journal of Fluid Mechanics*, 1990, **215,** 601–638.
11. Riley, J. J., Metcalfe, R. W. and Weissman, M. A., Direct numerical simulation of homogeneous turbulence in density stratified fluids. In *Proceedings of the American Institute of Physics*, Vol. 76, *Nonlinear Properties of Internal Waves*, ed. B. J. West. New York, 1981, pp. 79–112.
12. Lilly, D. K., Stratified turbulence and mesoscale variability of the atmosphere. *Journal of Atmospheric Science*, 1983, **40,** 749–761.
13. Metais, O., Influence of stable stratification on three-dimensional isotropic turbulence. *Proceedings of the 5th Symposium on Turbulent Shear Flows*. New York, 1985.
14. Metais, O. and Herring, J. R., Numerical simulation of freely evolving turbulence in stably stratified fluid influence of stable stratification on three-dimensional isotropic turbulence. *Proceedings of the 5th Symposium on Turbulent Shear Flows*. New York, 1985.
15. Hinze, J. O., *Turbulence. An Introduction to its Mechanism and Theory*. McGraw-Hill, New York, 1959.
16. Browand, F. K. and Hopfinger, E. L., The influence of vertical turbulent scale by stable stratification. In *Conference on Turbulence and Diffusion in Stable Environments*. Clarendon, Oxford, 1985.
17. Gerz, T. and Yamazaki, H., Direct numerical simulation of buoyancy-driven turbulence in stably stratified fluid. *Journal of Fluid Mechanics*, 1993, **249,** 415–440.
18. Rotta, J. C., Statistische Theorie nicht-homogeher Turbulenz. *Zurnal Physics*, 1952, **129,** 547–572.
19. Schuman, U. and Petterson, G. S., Numerical study of the return of axisymmetric turbulence to isotropy. *Journal of Fluid Mechanics*, 1978, **88,** 711–735.
20. Dunn, D. W. and Reid, W. H., Heat transfer in isotropic turbulence during final period of decay. NACA report, TN4186, 1958.
21. Nayfeh, A., *Perturbation Methods*. Wiley Interscience, New York, 1974.
22. Van Dyke, M., *Perturbation Methods in Fluid Mechanics*. Academic Press, New York, 1964.